Pyrene derived functionalized low molecular weight organic gelators and gels†

Arno Hahma,*[a] Shreedhar Bhat,[bc] Kimmo Leivo,[a] Juha Linnanto,[a] Manu Lahtinen[a] and Kari Rissanen[b]

Received (in Montpellier, France) 30th January 2008, Accepted 13th March 2008
First published as an Advance Article on the web 23rd April 2008
DOI: 10.1039/b801708e

Pyrene derived binary functionalized low molecular weight organic gelators (FLMOGs) and gels thereof in selected organic solvents were synthesized and characterized. The functionality refers to a functional group that does not take part in formation of the supramolecular gel network, but remains free and available for other purposes, such as to bind nanoparticles or other molecules into the gel structure.

Functional groups were observed to disturb gel formation strongly, if they interact with each other within the same supramolecule due to the formation of competitive structures. Preventing such interactions restored the original gel properties. A gel with weaker supramolecular bonding than the binding between the functional groups was successfully made by separating the functional groups by distance. The π–π-interaction was found to be of negligible significance to the supramolecular binding energy, but probably essential to align the molecules to a one-dimensional chain and bring them into the range of van der Waals forces mainly responsible for the binding in this system. Solvent was observed to increase the binding energy of the supramolecule.

All molecules were characterized by spectroscopic techniques and elemental analysis. Selected gels were characterized with rheometry, scanning electron microscopy, UV- and fluorescence spectroscopy. Gelation kinetics and hysteresis were measured by UV-spectroscopy and a fast gelation process was observed for all the gelators studied. The melting enthalpies were measured by DSC and calculated theoretically by PM3 level of theory.

Introduction

A low molecular weight organogel is an organic solvent with a considerable increase in viscosity by means of formation of a 3D-network of entangled supramolecular fibers, which are formed by the self-arrangement of small gelator molecules instead of a network of polymer chains. Aggregation of low molecular weight organic gelators (LMOGs) is usually driven by specific noncovalent intermolecular forces, such as π–π interaction, hydrogen-bond formation, metal coordination, solvo/hydrophobic, dipole–dipole or van der Waals interactions. All such interactions lead to a great diversity of possible organic gelators.[1] A large number of different organic gelators have been discovered serendipitously, but recently there has been a tendency to actively design new organic gelator molecules.[2]

The ease of formation and the reversibility of gelation by LMOGs are attractive strategies for synthesizing novel materials.[3] Material design is a highly competitive area of current research. Many of the reported materials are derived from complicated molecules[4] that are laborious to synthesize and expensive. In addition, many compounds are effective gelators, but do not have any functional groups to be used as binding sites to other materials, such as nanoparticles. In this context, pyrene based LMOGs and functionalized LMOGs are simple compounds, which have proved extremely effective in gelling many organic solvents in less than 1% w/w concentrations[5] as such or as mixtures. However, pyrene derived gelators investigated so far possess no functionality except van der Waals interactions to bind materials into the gel network or to control the gel structure.

In this paper we present a new class of very simple functionalized low molecular weight gelators (FLMOGs) derived from pyrene, which have the ability to effectively bind to polar surfaces and incorporate for instance metallic particles as an integral part of the gel structure yet forming a gel. The functional groups of choice are polar groups that readily bind to metal and metal oxide surfaces or react with metals to form covalent or ionic compounds. Functional groups such as carboxylic acid, alcohol, hydrazide and amine are especially suitable for this task in diminishing order of acidity. In addition, these functional groups can readily be used to bind other molecules to the gelator structure.

The application for the gelators in this study is to create gels that can bind particulate material, such as metal powders and metallic nanoparticles, into the gel network resulting in a stable gel, where the particles cannot sediment even under

---

[a] *Department of Chemistry, University of Jyväskylä, P.O. Box 35, FIN-40014 JYU, Finland. E-mail: arno@jyu.fi; Fax: +358 50 8428 5243; Tel: +358 50 428 5243*
[b] *Nanoscience Center, Department of Chemistry, University of Jyväskylä, P.O. Box 35, FIN-40014 JYU, Finland*
[c] *Department of Organic Chemistry, Indian Institute of Science, Bangalore, 560012, India*

† Electronic supplementary information (ESI) available: Experimental and characterization data, and photographs of the gels. See DOI: 10.1039/b801708e

severe acceleration. Unfortunately, all gelators based on any kind of strong polar interactions contain functional groups, which form the intermolecular bonds to form a gel. Those functional groups are usually reserved for forming the gel network and hence are not available to bind to other materials into the gel. Mixing adsorbent materials into such gels immediately destroys the gel if the surface of the extra material binds to the same functional groups that would otherwise form a gel. In order to use the gelator to bind other materials than the solvent it is essential to design a system that forms the gel by such interactions that do not bind readily to adsorbent surfaces, which are typically very polar compared to the organic solvent to be gelled. On the other hand, the functional groups attached to the gelator molecules have to bind strongly onto the surfaces in order to displace any gelator adsorbed from a wrong location or block the surfaces before the gelating site is adsorbed on them. This requirement excludes single component LMOGs, since there is not much control available over which functional group of the molecule binds to the adsorbent surface first. The classical pyrene based gelators[5] were found to be more tolerant to adsorbent materials, showed the best gelation properties and gels thereof were found to have excellent rheological properties and stability for application as fuel gelators. These materials were therefore selected as the base system to be extended to a group of functionalized gelators.

Results and discussion

Gelator syntheses

Compounds **1–11** (Scheme 1) were synthesized starting from pyrene by following a modified known route[5a] through Friedel–Crafts acylation using $TiCl_4$ catalyst, which furnished an ω-keto acid. The keto group was subsequently reduced by the Wolff–Kishner method into the corresponding methylene group and the acid group was then transformed into the appropriate functional groups. The reactants were chosen to have the desired functionality in advance (carboxylic, ester) or the carboxylic based functional group was transformed after the first attachment of the side chain to the corresponding alcohol, hydrazide and amine derivatives. All the new compounds were identified by spectroscopic techniques and elemental analysis.‡§ The synthesis is simple in principle, but the purification of the compounds containing functional groups may be difficult and requires chromatographic techniques in many cases, while non-functional gelators can be readily recrystallized from hexane after filtration through a short column of silica.

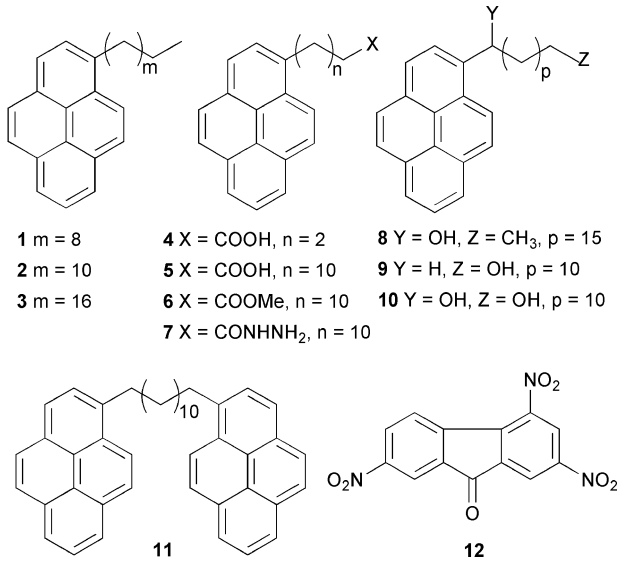

Scheme 1 Functional, pyrene based organic gelators with TNF.

Gels and gelation properties

All gel samples were prepared by adding equimolar amounts of gelator and 2,4,7-trinitrofluorenone (TNF, **12**, Scheme 1) to a solvent and heating, if necessary, up to the boiling point of the solvent, until at least the gelator, and preferably both compounds, were fully dissolved. The solution was allowed to cool down to room temperature, whereby the gel formed, if TNF was soluble enough (Fig. 1).

Gelation tests indicated that compounds **1–11** do not form gels alone in any of the organic solvents tested so far. However, all of these compounds do gel many organic solvents in the presence of TNF, if the gelator and TNF are sufficiently soluble. The results from the gelation experiments at 15 mmol kg^{-1} concentration (+TNF 15 mmol kg^{-1}) have been listed in Table 1 and shown in the ESI.† The gels are optically transparent but dark red or brown at low gelator and charge transfer (CT) agent concentrations (at and below 2% w/w). At higher concentration (above 3% w/w) the gels are translucent and contain dispersed CT agent particles inside the gel. When heated up to and above the melting point, the colour fades gradually and the solution becomes clear and pale yellow or colourless showing the breakup of the CT complex. The dark colour returns gradually upon cooling.

Compounds **1–11** formed the strongest gels in higher alcohols. For obtaining strong gels alcohols above 1-butanol have been found to be optimal. Dissolution in lower chain alcohols ($<C_5$) resulted in precipitation of the red CT complex in many cases. Compounds **1–3** gel even alkane solvents while compounds **4–11** are not soluble enough. This is partly due to the poor solubility of the CT agent TNF (**12**) in aliphatic hydrocarbons. Interestingly, compounds **1** and **2** were found to produce stable gels in petroleum ether in the presence of only a trace of TNF.§ These gels are stable, but lightly coloured and weaker than the 1 : 1 gelator TNF gels. This supports the observation that the CT mechanism is not the main source of binding energy, but nevertheless, without any CT agent no gel is formed and the CT mechanism is needed at least as an initiator.

The gelation properties of compounds **1–11** in 1-decanol have been studied in more detail. In 1-decanol, these compounds form optically transparent CT gels that are deep red in colour. The visually observed gel transparency† against a white illuminated background follows an order **9** > **6** > **7**

---

‡ Known compounds: **2**,[5a] but literature data incomplete: **4**,[8b] **5**–**6**.[8a]

§ CT-gels can also be obtained at lower ratios of CT-agent and pyrene analogs. We have found that as small as 5% doping is sufficient to gel petroleum ether (boiling range 80–100 °C) using compounds **1–3**.

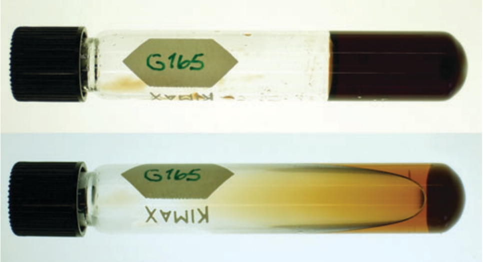

Fig. 1 Compound **5** in 1-octanol as gel at 25 °C (above) and as sol at 80 °C (below) at 30 mmol kg^{-1} gelator + 30 mmol kg^{-1} TNF concentration. The sol is lightly colored, the gel is dark red. The black shadow at the bottom of in the sol is a stirrer magnet.

$> \mathbf{5} > \mathbf{3} > \mathbf{2} > \mathbf{1}$, which agrees well with the gelator polarity. However, T_{gel} followed the reverse order, transparent gels melting at lower temperatures than the opaque gels.

The gels proved extremely stable to the effects of acceleration. Less than 1% of free solvent was released by centrifuging a 5 ml gel sample at 15 mmol kg^{-1} concentration in 1-octanol under 1000 *g* acceleration for one hour.

Thermoanalysis

DSC experiments were performed to study the melting behaviour of the CT complexes of **3**, **5** and **7** in 1-decanol at 15 mmol kg^{-1} concentration to determine the melting enthalpies (Fig. 2). The DSC profiles show several exothermic transitions along with the endothermic melting transition, showing that many structural changes take place in the material during heating. All these CT complexes melt in a relatively narrow temperature range (ranging from 65 to 75 °C) depending on the functional groups present on the pyrene system. At this stage we do not clearly understand the reason for the exothermic phase transitions observed by DSC and the melting enthalpies of complexes of compounds **3** and **4** could not be determined due to unexplained endothermic transitions, while compound **7** showed a clear endothermic peak. It should be noted, however, that these very small enthalpies are at the limits of the instrument, even though the measured curves were repeatable. The curves shown are an average of three runs. The enthalpy changes measured for these transitions are very low: +13 kJ mol^{-1} for compound **7** with 1 : 1 TNF. This is much less than the melting enthalpy of the pure gelator.

Table 1 Observations from gelation tests with TNF[a]

Gelator	Hexane	$CHCl_3$	C_6H_6	Toluene	Octanol	Decanol	Dodecanol
1	g	s	s	s	sg	sg	sg
2	g	s	s	s	g	sg	sg
3	g	s	s	s	g	sg	sg
4	i	s	s	s	wg	wg	wg
5	i	s	s	s	wg	sg	sg
5	i	s	s	s	wg	sg	sg
7	i	s	s	s	wg	wg	sg
8	i	s	s	s	wg	wg	g
9	i	s	s	s	wg	g	sg
10	i	s	s	s	wg	wg	g
11	i	s	s	s	wg	wg	wg

[a] 15 mmol kg^{-1} gelator, 15 mmol kg^{-1} TNF; sg = strong gel, g = gel, wg = weak gel, s = sol, i = solubility too small, otherwise would form a gel.

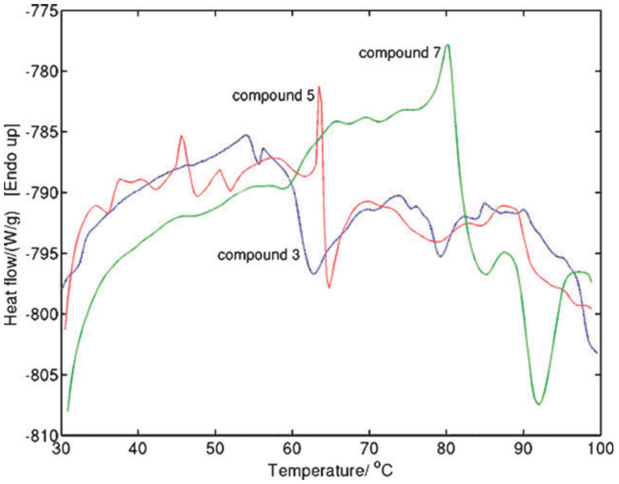

Fig. 2 DSC of gels made of compounds **3**, **5** and **7** in 1-decanol, 15 mmol kg^{-1} gelator, 15 mmol kg^{-1} TNF, heating rate: 20 °C min^{-1}.

Spectroscopic properties and gelation kinetics

Gelator molecules **1–11** are highly UV and fluorescence active. All these compounds show characteristic UV/visible absorption bands of pyrene. A very strong absorption band starting at 560 nm and extending to 360 nm was observed (Fig. 3) when the charge transfer agent TNF was added to sufficiently concentrated gelator solutions of **1–11** in 1-decanol. The absorption is very broad and all wavelengths at and below 550 nm are extremely strongly absorbed in the gel while the sol is at least partially transparent over the entire range. The broad absorption band is responsible for the deep red colour of the gels resulting from the CT complex. Note that the gel UV/Vis spectrum exceeds the device range due to the high concentration of the material in the gel (8 mmol kg^{-1}) from the point of view of the UV/Vis measurement. The samples

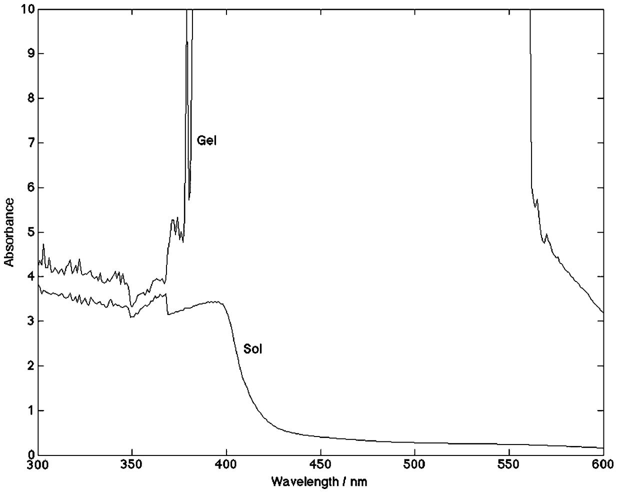

Fig. 3 UV/Vis spectrum of gel at 25 °C and sol at 80 °C made from compound **5** in 1-decanol at 8 mmol kg^{-1} gelator and 8 mmol kg^{-1} TNF concentration. The gel spectrum is over scale, but the gel could not be diluted more because it would break down at lower concentrations.

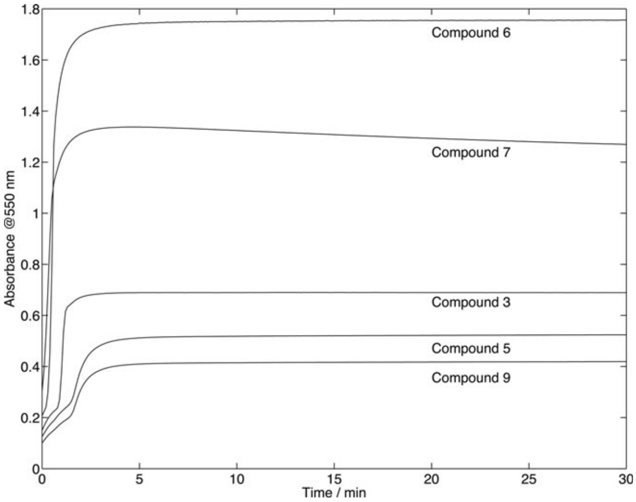

Fig. 4 Gelation kinetics of compounds **3**, **5** and **7** by UV/Vis in 1-decanol at 15 mmol kg^{-1} gelator and 15 mmol kg^{-1} TNF concentration.

could not be diluted more, since no gel forms at concentrations below 8 mmol kg^{-1} and no change in the spectrum is observed at lower concentrations than that. The kinetic measurements were carried out at 550 nm, *i.e.* at the edge of the absorption band to avoid exceeding the spectrometer range even in a gel state. Absorption and fluorescence maxima for the gel were at 480 nm, but this wavelength could not be used in UV/Vis or kinetic measurements due to excessive absorption.

The gelation kinetics for gels of **3**, **5–9** (Fig. 4) were studied by monitoring the charge transfer band. During the cooling process of a hot sol the initial change in the absorbance at 550 nm is very low for few seconds but is enhanced rapidly with cooling and reaches a maximum steady value at the gelling point, since the CT band is very sensitive to temperature. A kinetic plot indicated that the compounds **3**, **6** and **7** form CT gels twice as fast (2 min to steady absorption) as **5** and **9** (5 min) containing hydroxyl groups at the chain end. The effect of the finite cooling rate is negligible on this time scale, since cooling will only take a few seconds in the setup used. Nevertheless, all these compounds form gels very fast and the process is fully reversible unlike with many polymeric gelators, where re-equilibration can take days or weeks.

We carried out both melting and cooling studies of the gels of **6** with the help of the CT band. The hysteresis curve showed that the deaggregation process commences already at 35 °C upon heating while the aggregation starts at 55 °C during the cooling process (Fig. 5). A rather small hysteresis effect was observed despite the relatively fast heating and cooling rate (10 °C min^{-1}) also showing the gels form and equilibrate fast. The hysteresis results are in accordance with rheology measurements, which show the onset of the reduction of the storage modulus G' at around 40 °C. An example is presented for the compounds **1** and **5** in Fig. 6.

The pyrene ring fluoresces strongly and shows five emission bands at low concentrations. The third and first bands are highly sensitive to the dielectric constant of the solvent medium. At higher concentrations pyrene is expected to show an excimer band at 480 nm due to the formation of an excited state dimer. A broad fluorescence band was observed at 470–500 nm with excitation wavelength 336 nm. As the concentration increases the fluorescence properties of the molecule change and processes such as the internal filter effect and scattering may affect the fluorescence.

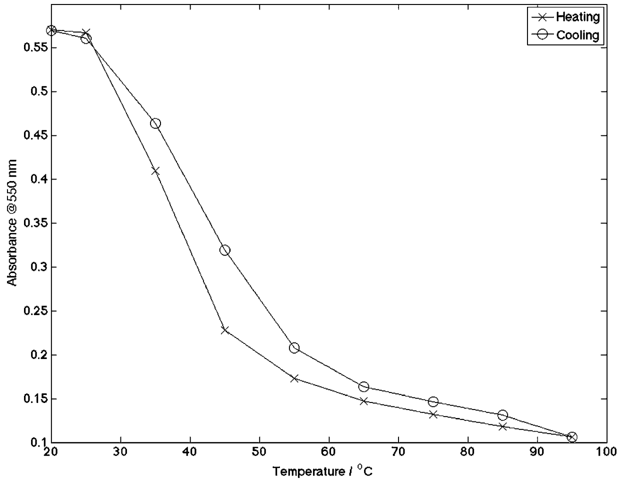

Fig. 5 Gelation hysteresis of compound **6** in 1-decanol by UV/Vis. Heating and cooling rates were 10 °C min^{-1}.

Although the UV/Vis and fluorescence experiments at higher concentrations are not recommended in general, they can give a general idea about the material properties. Therefore, the emissive properties of both sols and gels of compounds **1–11** have been studied, which showed a strong fluorescence (λ_{max} at 480 nm) resulting from the excited state complex with TNF (Fig. 7). The fluorescence intensity of the gels is also temperature dependent. The gel melts completely before 75 °C if determined by fluorescence. This is in accordance with visual T_{gel} values of the gels and with the results from the rheometry and UV/Vis experiments.

Rheological properties

Rheologically, the gels behave almost ideally as a function of temperature. First the storage modulus decays only slowly, but

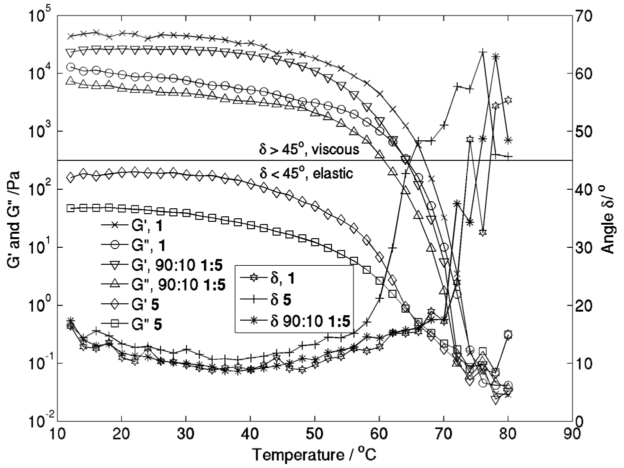

Fig. 6 Rheological properties of gels of compounds **1** and **5** in 1-octanol as a function of temperature. G' is the storage modulus, G'' is the loss modulus and δ is the phase angle of the stress *vs.* strain at 1 Hz frequency.

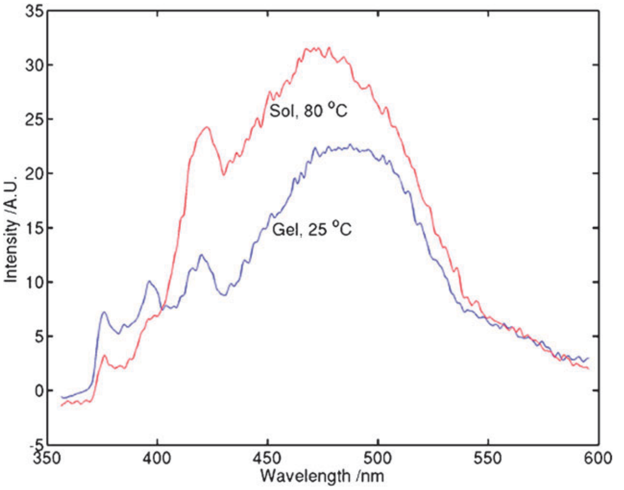

Fig. 7 Fluorescence spectra of sol at 80 °C and gel at 25 °C of compound **5** in 1-decanol at 15 mmol kg^{-1} gelator and 15 mmol kg^{-1} TNF. The excitation wavelength was 336 nm.

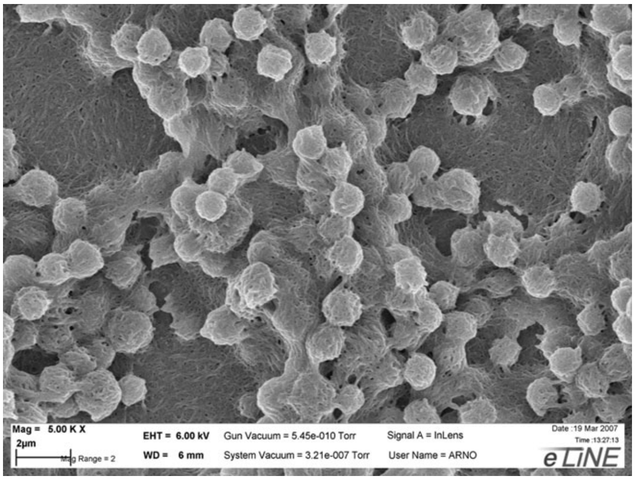

Fig. 8 Xerogel of compound **7** from 1-decanol has both fibrillar and granular structure.

drops sharply close to the melting point of the gel. The melting point is defined as the point where the phase angle reaches 45° (Fig. 6) and the material becomes more viscous than elastic. The functionalized gelator **5** is considerably weaker than the non-functionalized analog **1**, however, as a mixture the gel shows only a slight reduction of the storage modulus, probably due to different polarity and length of the side chains and not due to functional group interactions. At this concentration, every sixth molecule in the gelator chain has a functional group on average spacing the functional groups so far from each other that they no longer interact with adjacent groups within the same supramolecular chain preventing distortion of the supramolecular structure.

Xerogel structure

The xerogels were imaged with high resolution scanning electron microscopy (HR-SEM) to study the supramolecular structure of the gel. As an example, an HR-SEM image of **7** is presented in Fig. 8. The image showed an interconnected fiber network with evenly sized spherical clusters. The fibers were uniformly 50 nm and the clusters 1.5 μm in diameter. All gels showed an at least fibrous structure, but the diameter of the fibres varied from 20 nm to about 300 nm with different molecules: the longer the side chain in the pyrene nucleus, the thicker the fibres in the xerogel. A dual structure was observed in all gels from gelators with functional groups at the end of the side chain, *e.g.* in gels of **5–7** and **9**.

Gelation process

The exact mechanism for the gelation of pyrene analogs in the presence of TNF is not completely understood.§ TNF is used as a coupling reagent in the gelation and is presumed to help the one dimensional growth of the substituted pyrene molecules by forming a charge transfer complex with the pyrene nucleus. 1,3,5-Trinitrobenzene (TNB) also proved effective when used in a 2 : 1 molar ratio with the gelator. TNB-gels were opaque and bright orange in colour. With TNB, the aliphatic hydrocarbons can be more readily gelled due to the much better solubility of TNB. Complexing with 2,4,5,7-tetranitrofluorenone (TeNF) formed dark green, almost black gels,† which precipitated on standing within a few days showing the complex was too strong. Aromatic hydrocarbons could not be gelled with any combination, but they dissolved the compounds into a sol and prevented gelation by complexing to the CT agent themselves or by dissolving the resulting CT complex too well. Pyrene itself also forms a CT complex in organic solvents, but the gelation process requires a long alkyl chain (>7 CH_2) on the pyrene moiety. This alkyl chain provides rigidity to the 1D-aggregates and binds solvent molecules to the backbone of the gelator chain and increases solubility in aliphatic solvents.

Supramolecular structure and properties

The charge transfer complex enthalpy of formation of **7** was calculated with PM3 level of theory using Gaussian 03[6] in the gas phase at 0 K. Two possible structures with almost exactly the same energy of formation were found: a linear chain (ΔH_f = −7.4 kJ mol^{-1}) and a spherical aggregate (ΔH_f = −7.6 kJ mol^{-1}), in which the π–π-interactions are broken, but hydrogen bonding between –C=O and –$NHNH_2$ is established twisting the chain structure into a spheroid or helix (Fig. 9).

Calculations on larger than dimeric aggregates have been unsuccessful so far due to the very flat potential energy surface and due to the very large number of local minima in these systems. A similar dual structure is observed at a much larger scale in the SEM image (Fig. 8). Unfortunately, crystal structures of the CT complexes could not be determined so far and more rigorous evidence of the theoretically proposed dual structure could not be obtained.

The measured melting enthalpy of the CT complex of **7** by DSC is +13 kJ mol^{-1}. The difference from the calculated values at 0 K in the gas phase is surprisingly small, indicating that the gelator system has a low entropy change at its melting point and retains some of its ordered structure even in a molten state, or that adding solvent to the CT complex increases its bonding energy or both of the above.

Charge transfer

The sum of atom charges on TNF by MKS method was found to be −0.0055 electron charges in the linear chain and zero in the twisted structure showing the CT mechanism is weak and present only for the linear chain structure. Similar results have also been observed previously.[7] Less than 5% of the bonding energy in the linear chain structure is due to CT interaction, the rest being due to van der Waals bonding.

Consequently, the CT mechanism alone cannot be responsible for gelator chain formation nor the melting enthalpy observed. It may, however, be necessary to first align the molecules by π–π-interactions into the correct positions, where short range multipolar field coulombic interactions between individual atoms in the gelator and TNF can take over. Individual atoms in TNF have charges as much as ±0.5 and in the gelator molecule up to ±0.3 electron charges. Such charges create much larger bonding energies than 0.0055 total electron charge for the entire molecule despite the large surface area. In order for ideal atom-to-atom van der Waals bonding to occur, the atoms have to be aligned in such a way that a positively charged atom always matches a negatively charged counterpart in the adjacent molecule. Even a weakly electronegative substituent on the pyrene nucleus inhibits gelation, *e.g.* supramolecule formation, since it swaps the order of negative and positive atoms in the pyrene nucleus and the match with TNF at the optimal CT complex geometry is lost in addition to reduction of the π-electron density.

Solvent effects

The solvent was observed to increase the bonding energy of the complex as expected. The calculations were carried out without solvent molecules present while DSC was carried out with solvent producing approximately twice larger enthalpy than the calculations.

Hydrogen bonding

The alternative twisted structure bonding energy originates from hydrogen bonding only. As this configuration has only one binding site, it cannot form a gel network, but works to break such ordering, if present in the gel chain. The side chains in the supramolecule are located so far from each other (Fig. 9) that hydrogen bonding at the other end of the side chain twists the pyrenes apart despite the flexibility available in the side chain. Thus, hydrogen bonding between the side chains should be prevented by keeping the functional groups apart. This is necessary also, since the functional groups are not available for binding other materials, if they coordinate to each other. The solution to this is to add enough non-functionalized pyrene based gelator or even neat pyrene to the mixture to separate the hydrogen bonding groups to at least two pyrene–TNF-units apart preventing mutual interactions. This approach proved very effective as seen in Fig. 6 and a LMOG based gel with large amounts of free and sterically unhindered functional groups could be made.

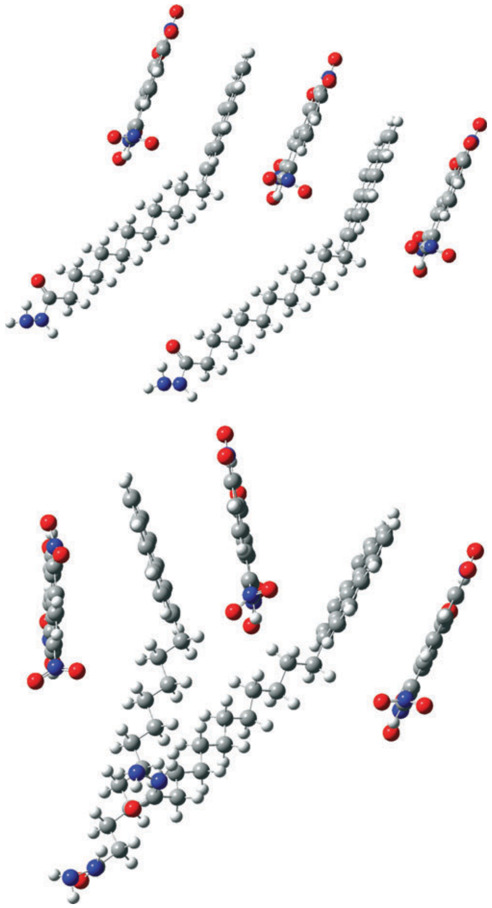

Fig. 9 Two possible minimum energy structures of compound **7** with TNF: linear π–π-configuration (above) and hydrogen bonded helical or spherical aggregate (below).

Conclusions

We have successfully implemented a group of pyrene based functionalized low molecular weight organic gelators (FLMOGs) and shown that it is possible to make a gel with free, unhindered functional groups available as binding sites to other molecules and materials. We have implemented a gel that forms with a weaker bonding mechanism than the gelator functional groups can bond with. We have also shown that such gelator systems are not allowed to contain structurally competing intermolecular binding sites within a single supramolecule or the resulting gels become weak and behave unpredictably (Fig. 6). In addition, the first atom of the side chain attached to the pyrene nucleus may not have substituents other than hydrogen or the formation of gel will be inhibited due to steric effects, even though such substituents were favourable to the formation of the CT complex (electron donating groups) (Table 1). If the pyrene substituent is electron withdrawing it causes unfavourable charge distribution in the pyrene nucleus at optimal CT complex geometry preventing gelation.

The adverse effects of the gelator functionality can be controlled by mixing non-functionalized and functional gelators or to a limited amount even pyrene to effect a supramolecular copolymer (Fig. 6) and also by crosslinking the gel at supramolecular level with compound **11** in analogy to polymer chemistry separating functional groups from each other within an individual gelator supramolecule. We have also shown that charge transfer mechanism plays only a minor role as far as the total agglomeration energy of the gelator is concerned. It may, however, be essential to have π–π- and CT complexation to align the molecules correctly for the van der Waals forces to take over the main binding role. The solvent increases the supramolecular binding energy compared to the corresponding vacuum structure, as expected.

Experimental

Spectral characterizations

Compounds. NMR spectra were recorded with Bruker Avance DPX 250 (250 MHz) or Bruker Avance DRX 500 (500 MHz). The solvent peak in ^{13}C-NMR was adjusted to 77.23 ppm for $CDCl_3$ and to 39.51 ppm for DMSO-d_6 at 30 °C. *J* values are given in Hz. Mass spectra were measured with Micromass LCT (electrospray MS) or with VG AutoSpec (electron impact MS). The reference material used for high resolution mass spectroscopy (HRMS) was leucine enkephalin acetate hydrate for ESI-MS and perfluorokerosene for EI-MS.

Gels

The gel transparency and turbidity were estimated visually against a background lighted table. A photograph of this experiment can be found in the ESI.†

UV/Vis and fluorescence spectra were recorded in a 10 × 10 mm thermostated quartz cuvette at 25 °C using Shimadzu UV-2100 UV/Vis spectrophotometer. The hysteresis studies were carried out with the same instrument with a heating and cooling rate of 10 °C per minute.

The kinetic experiments by UV-spectroscopy were carried out by transferring a hot sol (at 80 °C) consisting of a gelator and TNF in a 2 : 1 ratio into a UV cuvette with path length 1 mm maintained at 25 °C. Less TNF than a 1 : 1 ratio was used to prevent precipitation of any substance and to reduce the already very high absorbance level. Absorbance at 550 nm was monitored against time. Fluorescence spectra were measured using Perkin-Elmer LS-50B luminescence spectrometer with a 10 mm path length quartz cuvette at 25 °C using 336 nm excitation wavelength.

Thermoanalysis

Thermal transitions for the gels were determined on power compensation type Perkin-Elmer Pyris Diamond DSC. The measurements were carried out under nitrogen atmosphere (flow rate 50 ml min^{-1}) using 50 μl sealed aluminium sample pans. The gel samples were melted in a test tube by heating it with a hot air gun to 100–130 °C and a droplet of the molten gel was then quickly placed on the sample pan, which was allowed to cool to room temperature before sealing the pan. The temperature calibration of DSC was made using two standard materials (*n*-decane, indium) and energy calibration by an indium standard (28.45 J g^{-1}). Each sample was heated from 25 to 100 °C with a heating rate of 20 °C min^{-1}. Sample weights of 10–20 mg were used on the measurements. The uncertainty for measured temperatures was less than 0.8 °C for all measurements.

Rheology

Rheological properties were measured with Haake Rheostress1 rheometer using a cone–plate configuration. The sample was spread over the measurement disc thermostated at 10 °C. The measurement head (35 mm diameter 2° titanium cone, type C35/2 Ti) was lowered on to the sample slowly by the control software squeezing excess gel out of the gap. Oscillatory mode measurement was started immediately the measurement head reached its position, since lowering the head took about one minute allowing the gel to cool down in time. Constant frequency of 1 Hz and constant stress of 1 Pa were used while sweeping the temperature from 10 °C up to 80 °C within one hour, *e.g.* at a rate of 1.17 °C per minute. The stress level was chosen according to prior stress sweep measurements to a linear range of the modulus *vs.* stress dependency within the entire temperature range of interest. A PTFE cover was placed over the measurement head to prevent condensation of moisture at low temperatures and evaporation of the solvent at the high temperature end. Three parallel measurements were carried out and the average of the three was used as the final result. Stray points were removed from the data prior to averaging, if the said points were clearly erratic.

The storage and loss modulus and the phase angle were automatically calculated by the Haake Rheowin v3.21 controlling software according to calibrations of the instrument. The temperature was swept upwards in order to have the gel as intact as possible at the beginning of the measurement and avoid melting it prematurely. Additionally, the samples were stored overnight at room temperature before measuring them to ensure the gel had fully cured and an equilibrium state had been reached.

Microscopy

The gels were imaged with RAITH E-Line high resolution field emission scanning electron microscope equipped with Schottky tungsten field effect emitter. The samples were prepared on pieces of silicon wafers by melting 1 to 3 mg of gel on the wafer, cooling and drying at room temperature in an air stream for 3 days. The samples were then gold coated with sputtering with Jeol Fine Coat Ion Sputter JFC-1100. A sputtering time of 30 sec up to 1 min was used with 1 kV voltage, 10 mA of current and 5 mbar air as the gas medium producing a gold coating less than 1 nm thick on average. The samples were imaged using an aperture size of 10 or 30 μm, collector current 100 μA, spot size 20 nm, acceleration voltage 6 kV, working distance 6 mm and using ultra high vacuum ($<4 \times 10^{-7}$ Torr) with an Everhart Thornley in-lens detector.

Chemicals

All chemicals and solvents were used as received from sealed containers. The list of chemicals and their sources are given in the ESI.†

Syntheses

1-(Pyren-1-yl)decan-1-one (1a). Decanoic acid (86 g, 0.5 mol) was first treated with an excess of thionyl chloride (300 ml, 4.2 mol) and refluxed for 3–4 h. Excess of $SOCl_2$ was removed by distillation under reduced pressure. The decanoyl chloride (95 g, 0.5 mol) was mixed with pyrene (101 g, 0.5 mol) and 1,2-dichloroethane (DCE, 1200 ml). To this mixture was added $TiCl_4$ (150 g, 0.75 mol) dropwise with stirring, in an ice bath at below 5 °C, during the addition. The brown complex formed was stirred for a further 16 h at RT. The brown complex was cleaved by the addition of water and DCE was distilled off. The product was extracted into chloroform in a Soxhlet (1500 mL) and washed with water, saturated sodium bicarbonate (2 × 100 mL) and finally with water. The chloroform layer was dried over anhydrous $MgSO_4$ and concentrated under reduced pressure. The crude material was purified by recrystallization from hexane–chloroform 99–1. The pure product **1a** (156 g, 84%) was isolated as yellow solid; mp. 59–61 °C (Found: C, 87.96; H, 7.86. Calc. for $C_{26}H_{38}O$: C, 87.60; H, 7.92%); ν_{max}(KBr)/cm^{-1} 3045, 2920, 1594, 1506, 1466, 1413, 1382, 1254, 1218, 1182, 1063, 958, 842 and 714; δ_H/ppm (500 MHz; $CDCl_3$) 0.88 (3 H, t, 7.0), 1.29 (10 H, m), 1.46 (2 H, m), 1.87 (2 H, q, 7.5), 3.20 (2 H, t, 7.5), 7.97–8.35 (8 H, m) and 8.86 (1 H, d, 9.5); δ_C/ppm (126 MHz; $CDCl_3$) 14.06, 22.64, 25.03, 29.26, 29.43, 29.46, 29.49, 31.86, 42.74, 123.99, 124.40, 124.84, 124.92, 125.05, 125.91, 125.92, 126.13, 126.34, 127.08, 127.37, 129.23, 129.33, 129.41, 130.61, 131.13, 133.08, 133.54 and 205.44; HRMS: *m*/*z* (TOF-ES+) 357.2237 (Calc. for: $C_{26}H_{28}O + H$ 357.2216).

1-Decylpyrene (1). 1-(Pyren-1-yl)decan-1-one **1a** (148 g, 0.4 mol) and KOH (90 g, 1.6 mol) were mixed with digol (800 ml) and warmed to 180 °C. The solution turned brownish in colour. To this solution hydrazine monohydrate (40 ml, 0.8 mol) was added slowly keeping the temperature at 190–200 °C under a nitrogen atmosphere for 12 h. Finally, the temperature was slowly raised to 220 °C. Vapours were flushed out with nitrogen flow. The mixture was cooled to 50 °C. The product was extracted into 3 × 1000 ml hexane, which were filtered through 50 g of silica and dried over anhydrous $MgSO_4$. The combined extracts were evaporated to 1000 ml volume and left to crystallize over 3 days at RT. Additional crop was obtained by evaporating the hexane down to 400 ml and crystallizing overnight with seed crystals from the first batch. The pure product **1** (125 g, 88%) was obtained as bright yellow solid; mp 69–71 °C (Found: C, 91.09; H, 8.92. Calc. for $C_{26}H_{30}$: C, 91.17; H, 8.83%); ν_{max}(KBr)/cm^{-1} 3039, 2954, 2917, 2850, 1463, 961, 841, 824, 760, 722, 707, 680 and 625; δ_H/ppm (500 MHz; $CDCl_3$) 0.88 (3 H, t), 1.2-1.35 (10 H, m), 1.38 (2 H, m), 1.50 (2 H, q), 1.85 (2 H, q), 3.33 (2 H, t), 7.87 (1 H, d, J 8.0), 7.97–8.20 (7 H, m) and 8.29 (1 H, d, *J* 9.0 Hz); δ_C/ppm (126 MHz; $CDCl_3$) 14.10, 22.68, 29.34, 29.60, 29.636, 29.644, 29.84, 31.91, 31.93, 33.60, 124.57, 124.73, 124.75, 125.107, 125.114, 125.70, 126.44, 127.04, 127.19, 127.52, 128.62, 129.70, 130.97, 131.48 and 137.35; HRMS: *m*/*z* (EI 70 eV) 342.2355 (Calc. for $C_{26}H_{30}$: 342.2348).

1-Dodecylpyrene (2). Synthesis and characterization from ref. 5*a*; mp 72–73 °C (Found: C, 90.95; H, 9.33. Calc. for $C_{28}H_{34}$: C, 90.75; H, 9.25%); ν_{max}(thin film)/cm^{-1} 1465 and 840; δ_H/ppm (300 MHz; $CDCl_3$) 0.88 (3 H, t, J 6.8), 1.26–1.37 (16 H, m), 1.37 (2 H, q, *J* 7.5 Hz), 1.49 (2 H, m), 3.33 (2 H, t, J 7.7), 7.87 (1 H, d, J 7.8), 8.02 (2 H, m), 8.17 (5 H, m) and 8.29 (1 H, d, *J* 9.3 Hz); δ_C/ppm (75 MHz; $CDCl_3$) 22.07, 29.36, 29.61, 29.65, 29.68, 29.85, 31.93, 31.98, 33.64, 123.55, 124.59, 124.76, 124.77, 125.08, 125.74, 126.46, 127.07, 127.25, 127.54, 129.68, 130.96, 131.47 and 137.39; LRMS: *m*/*z* 384 (M^+).

1-(Pyren-1-yl)octadecan-1-one (3a). Stearic acid (4 g, 14.12 mmol) was first treated with excess of thionyl chloride (2.5 g, 21.2 mmol) and refluxed for 3–4 h. Excess of $SOCl_2$ was removed by distillation. The stearoyl chloride (3.6 g, 11.9 mmol) was mixed with pyrene (2 g, 9.9 mmol) and DCE (10 ml). To this mixture was added $TiCl_4$ (2.25 g, 11.9 mmol) dropwise with stirring over an ice bath. The temperature was maintained below 5 °C during the addition. The brown complex formed was stirred for further 12 h. The brown complex was cleaved by the addition of water and dilute HCl. The product was extracted into DCM (20 mL) and washed with saturated sodium bicarbonate (2 × 85 mL), dil. HCl and finally with water. The DCM layer was dried over anhydrous Na_2SO_4 and concentrated under reduced pressure. The crude material was purified further by chromatography over Merck 60 silica gel using DCM–hexane (1 : 9) as eluent. The pure product **3a** (3.25 g, 70%) was isolated as yellow solid; mp 74–76 °C (Found: C, 87.09; H, 9.47. Calc. for $C_{34}H_{44}O$: C, 87.12; H, 9.46%); ν_{max}(KBr)/cm^{-1} 2953–2849, 1672, 1471, 843 and 716; δ_H/ppm (250 MHz; $CDCl_3$) 0.88 (3 H, t, *J* 6.75 Hz), 1.25 (30 H, br s), 1.86 (2 H, m), 3.21 (2 H, t, J 7.5), 8.00–8.33 (8 H, m) and 8.87 (1 H, d, *J* 9.3 Hz); δ_C/ppm (63 MHz; $CDCl_3$) 14.11, 22.69, 25.03, 29.36, 29.44, 29.50, 29.62, 29.66, 29.70, 31.93, 42.73, 123.99, 124.40, 124.84, 125.04, 125.92, 126.13, 126.34, 127.08, 129.24, 129.33, 129.42, 130.60, 131.12, 133.05, 133.54 and 205.43; HRMS: *m*/*z* (EI 70 eV) 469.3383 (Calc. for $C_{34}H_{44}O$: 469.3426).

1-Octadecylpyrene (3). 1-(Pyren-1-yl)octadecan-1-one **3a** (0.5 g, 1.07 mmol) was mixed with KOH (0.36 g, 6.4 mmol) and digol (2 mL) and warmed to 110 °C. The hydrazine hydrate was then added dropwise to the above stirring mixture. This was stirred at 120 °C for 2–3 h. The temperature of the reaction was raised to 200 °C. After 1 h the reaction mixture was cooled to room temperature. The mixture was acidified with dil. HCl till neutral to litmus. The product was extracted in to chloroform and washed with saturated sodium bicarbonate (2 × 85 mL), dil. HCl and finally with water. The DCM layer was dried over anhydrous Na_2SO_4 and concentrated under reduced pressure. The crude material was purified further by chromatography over Merck silica 60 using hexane as eluent. The pure product **3** (0.34 g, 70%) was isolated as white solid; mp 83–84 °C (Found: C, 89.57; H, 10.27. Calc. for $C_{34}H_{46}$: C, 89.80, H, 10.19%); ν_{max}(KBr)/cm^{-1} 3039, 2965–2849, 1463 and 840; δ_H/ppm (250 MHz; $CDCl_3$) 0.89 (3 H, t, J 6.8), 1.26 (30 H, br s), 1.85 (2 H, m), 3.34 (2 H, t, *J* 7.5 Hz), 7.87 (1 H, d, J 7.8), 7.95–8.18 (7 H, m) and 8.29 (1 H, d, J 9.3); δ_C/ppm (63 MHz; $CDCl_3$) 14.11, 22.70, 29.37, 29.61, 29.71, 29.85, 31.94, 33.62, 123.54, 124.59, 124.75, 125.12, 125.73, 126.46, 127.06, 127.23, 127.54, 128.63, 129.70, 130.98, 131.49 and 137.38; HRMS: *m*/*z* (EI 70 eV) 454.3595 (Calc. for $C_{34}H_{46}$: 454.3599).

4-Oxo-4-(pyren-1-yl)butanoic acid (4a). Succinic acid (0.4 g) was refluxed with excess of acetic anhydride (5 mL) for 10 h. After the reaction acetic anhydride and acetic acid were removed by distillation. A mixture containing pyrene (0.5 g, 2.5 mmol) and succinic anhydride (about 0.39 g, 3 mmol) were dissolved in DCE (3 mL) and kept stirring on an ice bath. To this stirring solution $TiCl_4$ (0.56 g, 3 mmol) was added dropwise for 5 min and the stirring was continued for 24 h. The complex was hydrolyzed by the addition of water and dil. HCl. The product formed was extracted into EtOAc (15 mL) and washed with water (2 × 5 mL). The organic layer was dried over anhydrous Na_2SO_4 and concentrated under reduced pressure. The final product was further purified by chromatography over Merck silica 60 using acetone–DCM (1 : 9) as eluent. The pure product **4a** (0.51 g, 68%) was obtained as pale yellow crystalline solid; mp 184–185 °C (Found: C, 78.80; H, 4.52. Calc. for $C_{20}H_{13}O_3 + \frac{1}{4}H_2O$: C, 78.55; H, 4.28%); ν_{max}(KBr)/cm^{-1} 3453, 1695, 1665 and 842; δ_H/ppm (250 MHz; DMSO-d6) 2.76 (2 H, t, *J* 6.0 Hz), 3.49 (2 H, t, *J* 6.0 Hz), 8.12–8.43 (7 H, m), 8.57 (1 H, d, *J* 8.3 Hz) and 8.77 (1 H, d, *J* 9.5 Hz); δ_C/ppm(63 MHz; DMSO-d6) 28.55, 36.92, 123.47, 123.96, 124.44, 125.97, 126.39, 126.44, 126.72, 127.15, 128.12, 129.14, 129.29, 129.94, 130.63, 132.48, 133.01, 173.89 and 203.18; HRMS: *m*/*z* (TOF-ES−) 301.0365 (Calc. for $C_{20}H_{14}O_3$ − H: 301.0865).

4-(Pyren-1-yl)butanoic acid (4). To a reaction mixture containing 4-oxo-4-(pyren-1-yl)butanoic acid **4a** (0.5 g, 1.65 mmol), digol (2.0 mL) and KOH (0.74 g, 13.2 mmol) at 110 °C was added hydrazine monohydrate (0.83 g, 16.5 mmol) slowly and stirred for 2 h at 120 °C. The temperature of the reaction was increased to 180 °C with continued stirring for at least 50 min. The reaction mixture was poured into an ice bath and acidified until neutral to litmus and extracted with ethyl acetate (15 mL, 3 × 5 mL). The organic layer washed with water (2 × 5 mL) and dried over anhydrous Na_2SO_4. The crude product was further purified by column chromatography over Merck silica 60 using acetone–DCM (5 : 95) as eluent. The final product **4** (0.31 g, 65%) was obtained as pale yellow solid; mp 182–183 °C (Found: C, 80.41; H, 5.42. Calc. for $C_{20}H_{16}O_2 + \frac{1}{2}H_2O$: C, 80.84; H, 5.76%); ν_{max}(KBr)/cm^{-1} 3433, 2920, 2845, 1701 and 843; δ_H/ppm (250 MHz; $CDCl_3$) 2.22 (2 H, m), 2.52 (2 H, t, *J* 7.0 Hz), 3.43 (2 H, m), 7.87 (1 H, d, *J* 7.8 Hz), 7.95–8.20 (7 H, m) and 8.30 (1 H, d, *J* 9.3 Hz); δ_C/ppm (63 MHz; $CDCl_3$) 26.53, 32.68, 33.27, 123.25, 124.83, 124.86, 124.97, 125.03, 125.17, 125.88, 127.37, 127.50, 128.79, 130.09, 130.94, 131.46, 135.49 and 177.69; HRMS: *m*/*z* (EI 70 eV) 288.1145 (Calc. for $C_{20}H_{16}O_2$: 288.1150).

12-Oxo-12-(pyren-1-yl)dodecanoic acid (5a). Dodecanedioic acid (23 g, 0.1 mol) was first treated with excess of thionyl chloride (50 ml, 0.7 mol) and refluxed for 3–4 h. Excess of $SOCl_2$ was removed by distillation under reduced pressure. The dodecanedioyl dichloride was used without further purification.

To a reaction mixture containing pyrene (10 g, 49.5 mmol) and dodecanedioyl dichloride (14 g, 52.4 mmol) in DCE (20 mL) was cooled in an ice bath for 15 min. To this stirring solution $TiCl_4$ (5.7 g, 52 mmol) was added dropwise for 20 min. The dark brown complex formed was allowed to warm to room temperature. The stirring was continued until the starting material disappeared by TLC. The complex was cleaved by the addition of water and the product was extracted into $CHCl_3$. Washed with water (2 × 5 mL) and dried over anhydrous Na_2SO_4. The solvent was removed under reduced pressure. The product was further purified by chromatography over Merck silica 60 using acetone–DCM (1 : 9) as eluent. The pure product **5a** (5.0 g, 25%) was obtained as pale yellow solid; mp 116–117 °C (Found: C, 50.27; H, 8.20. Calc. for $C_{28}H_{30}O_3 + 14H_2O$: C, 50.43; H, 8.76%); ν_{max}(KBr)/cm^{-1} 3425, 3043, 2924, 2889, 2848, 1716, 1666 and 843; δ_H/ppm (250 MHz; DMSO-d6) 1.18 (10 H, br s), 1.26–1.45 (4 H, m), 1.71 (2 H, m), 2.14 (2 H, t, *J* 7.5 Hz), 3.22 (2 H, t, *J* 7.0 Hz), 8.09–8.39 (7 H, m), 8.50 (1 H, d, *J* 8.0 Hz) and 8.70 (1 H, d, *J* 9.3Hz); δ_C/ppm (63 MHz; DMSO-d6) 24.38, 24.48, 28.52, 28.61, 28.68, 28.79, 28.83, 33.67, 42.00, 123.56, 124.06, 124.36, 124.47, 125.99, 126.43, 126.45, 126.77, 127.20, 128.15, 129.22, 129.27, 129.99, 130.68, 132.88, 132.96, 174.51 and 205.09; HRMS: *m*/*z* (TOF-ES−) 413.2171 (Calc. for $C_{28}H_{30}O_3$ − H: 413.2117).

12-(Pyren-1-yl)dodecanoic acid (5). 12-Oxo-12-(pyren-1-yl)-dodecanoic acid **5a** (0.3 g, 0.7 mmol) and KOH (0.3 g, 5.5 mmol) were mixed with digol (1 ml) and warmed to 110 °C the solution turned brownish in colour. To this solution hydrazine monohydrate was added slowly and stirred at 120 °C for 2–3 h. Then the temperature was slowly raised to 200 °C. All the vapours were allowed to escape out under nitrogen flow. The mixture was cooled to room temperature and acidified with dil. HCl till neutral to litmus. The product was extracted into EtOAc, washed with water (2 × 5 ml) and dried over anhydrous Na_2SO_4. The crude product was concentrated to dryness under reduced pressure. The product was further purified by chromatography over Merck silica 60 using acetone–DCM (5 : 95) as eluent. The pure product **5** (0.19 g, 67%) was obtained as pale yellow solid; mp 110–111 °C (Found: C, 80.52; H, 7.72. Batch 1: calc. for $C_{28}H_{32}O_2 + H_2O$: C, 80.35; H, 8.18. Found: C, 82.58; H, 7.96. Batch 2: calc. for $C_{28}H_{32}O_2 + \frac{1}{2}H_2O$: C, 82.20; H, 8.12%); ν_{max}(KBr)/cm^{-1} 3435, 2921, 2846, 1705 and 844; δ_H/ppm (500 MHz; $CDCl_3$) 1.27 (10 H, br s), 1.38 (2 H, t, 7.5), 1.49 (2 H, q, 7.5), 1.63 (2 H, q, 7.5), 1.86 (2 H, q, 8.0), 2.34 (2 H, t, *J* 7.5 Hz), 3.34 (2 H, t, 8.0), 7.87 (1 H, d, *J* 8.0 Hz), 7.96–8.17 (7 H, m) and 8.29 (1 H, d, *J* 9.5 Hz); δ_C/ppm (126 MHz; $CDCl_3$) 24.67, 29.03, 29.19, 29.38, 29.54, 29.55, 29.56, 29.79, 31.92, 33.60, 33.88, 123.53, 124.59, 124.75, 124.76, 125.10, 125.11, 125.73, 126.45, 127.06, 127.23, 127.53, 128.62, 129.70, 130.97, 131.48, 137.35 and 179.21; HRMS: *m*/*z* (TOF-ES−) 399.2137 (Calc. for $C_{28}H_{32}O_2$ − H: 399.2324).

Methyl-12-(pyren-1-yl)dodecanoate (6). 12-(Pyren-1-yl)dodecanoic acid **5** (0.3 g, 0.75 mmol) was added to a solution containing 2 ml MeOH and 0.2 ml H_2SO_4 and refluxed for 4–5 h. After the completion, the reaction the mixture was neutralized with saturated $NaHCO_3$ and extracted into $CHCl_3$. The chloroform layer was washed with water (2 × 5 ml), dried over anhydrous Na_2SO_4. The solvent was removed under reduced pressure and purified further by column chromatography over Merck silica 60 using $CHCl_3$–hexane (2 : 8) as eluent. The pure product **6** (0.28 g, 90%) was obtained as pale yellow solid; mp 57.5–58.0 °C (Found: C, 84.02; H, 8.31. Calc. for $C_{29}H_{34}O_2 + \frac{1}{2}H_2O$: C, 84.01; H, 8.27%); ν_{max}(KBr)/cm^{-1} 3455, 3040, 2928, 2852, 1741, 1155 and 841; δ_H/ppm (500 MHz; $CDCl_3$) 1.29 (10 H, br s), 1.39 (2 H, m), 1.50 (2 H, q, 7.5), 1.63 (2 H, m), 1.87 (2 H, q, *J* 7.5 Hz), 2.31 (2 H, t, *J* 7.5 Hz), 3.34 (2 H, t, *J* 8.0 Hz), 3.68 (3 H, s), 7.87 (1 H, d, J 7.8), 7.97–8.17 (7 H, m) and 8.29 (1 H, d, *J* 9.0 Hz); δ_C/ppm (126 MHz; $CDCl_3$) 24.94, 29.12, 29.21, 29.40, 29.54, 29.55, 29.56, 29.79, 31.90, 33.57, 34.09, 51.36, 123.50, 124.56, 124.72, 124.74, 125.08, 125.09, 125.70, 126.43, 127.04, 127.19, 127.51, 128.60, 129.68, 130.95, 131.46, 137.31 and 174.26; HRMS: *m*/*z* (EI 70 eV) 414.2551 (Calc. for $C_{29}H_{34}O_2$: 414.2558).

12-(Pyren-1-yl)dodecanehydrazide (7). To a solution containing methyl-12-(pyren-1-yl)dodecanoate **6** (0.25 g, 0.6 mmol) in 3 mL methanol was added hydrazine hydrate (0.21 g, 4.2 mmol) and refluxed for 4 h. After the reaction the mixture was extracted into chloroform. The chloroform layer was washed with water (2 × 5 ml) and dried over anhydrous Na_2SO_4. Chloroform was removed under reduced pressure. The crude material was purified further by column chromatography over Merck silica 60 using acetone–DCM (1 : 9) as the eluent. The pure product **7** (0.21 g, 80%) was obtained as white solid; mp 122–123 °C (Found: C, 79.97; H, 8.113; N, 6.39. Calc. for $C_{28}H_{34}N_2O + \frac{1}{2}H_2O$: C, 79.50; H, 8.33; N, 6.61%); ν_{max}(KBr)/cm^{-1} 3430, 3300, 2918, 2850, 1631, 1530 and 842; δ_H/ppm (500 MHz; $CDCl_3$) 1.27 (10 H, br s), 1.38 (2 H, m), 1.48 (2 H, m), 1.60 (2 H, m), 1.86 (2 H, q, 7.5), 2.12 (2 H, t, *J* 8.0 Hz), 3.34 (2 H, t, *J* 8.0 Hz), 3.88 (2 H, br s), 6.60 (1 H, br s), 7.87 (1 H, d, *J* 8.0 Hz), 7.96–8.17 (7 H, m) and 8.28 (1 H, d, *J* 9.5 Hz); δ_C/ppm (126 MHz; $CDCl_3$) 25.47, 29.25, 29.41, 29.54, 29.55, 29.79, 31.93, 33.60, 34.59, 123.54, 124.60, 124.77, 125.11, 125.13, 125.75, 126.47, 127.07, 127.24, 127.54, 128.64, 129.71, 130.98, 131.49 and 137.36; HRMS: *m*/*z* (TOF-ES+) 415.2757 (Calc. for $C_{28}H_{34}N_2O$ + H: 415.2749).

1-(Pyren-1-yl)octadecan-1-ol (8). 1-(Pyren-1-yl)octadecan-1-one **3a** (0.1 g, 0.21 mmol) was dissolved in 1 mL of dry THF. This solution was added dropwise to a stirring suspension of LAH (0.08 g, 2.1 mmol) in 1 mL of dry THF. The resulting mixture was stirred for 3–4 h at RT. After the reaction, excess of LAH was neutralized by addition EtOAc and moist EtOH. The mixture was filtered and filtrate was concentrated and dried. The crude product was further purified by column chromatography over Merck silica 60 column using EtOAc–DCM (5 : 95) as eluent. The pure product **8** (0.072 g, 72%) was isolated as a pale yellow powder; mp 85–87 °C (Found: C, 85.89; H, 9.90. Calc. for $C_{34}H_{46}O + \frac{1}{4}H_2O$: C, 85.93; H, 9.81%); ν_{max}(KBr)/cm^{-1} 3440, 2920, 2850, 1466, 1055 and 842; δ_H/ppm (250 MHz; $CDCl_3$) 0.88 (3 H, t, 6.8), 1.24–1.61 (30 H, m), 2.00–2.13 (2 H, m), 5.79 (1 H, t, 6.5), 7.95–8.20 (8 H, m) and 8.36 (1 H, d, *J* 9.3 Hz); δ_C/pppm (63 MHz; $CDCl_3$) 14.33, 22.91, 26.49, 29.58, 29.92, 32.15, 39.42, 71.67, 122.79, 123.55, 125.14, 125.20, 125.21, 125.27, 125.43, 126.13, 127.40, 127.72, 127.77, 127.81, 130.84, 130.93, 131.66 and 138.68; HRMS: *m*/*z* (TOF-ES+) 493.2900 (Calc. for $C_{34}H_{46}ONa$: 493.3446).

12-(Pyren-1-yl)dodecan-1-ol (9). Methyl-12-(pyren-1-yl)dodecanoate **6** (0.1 g, 0.24 mmol) was dissolved in 1 mL of dry THF. This solution was added dropwise to a stirring suspension of LAH (0.092 g, 2.4 mmol) in 1 mL of dry THF. The resulting mixture was stirred for 3–4 h at RT. After the reaction, the excess of LAH was neutralized by addition EtOAc and moist EtOH. The mixture was filtered. Filtrate was concentrated and dried. The crude product was further purified by column chromatography over Merck silica 60 column using DCM–EtOAc (98 : 2) as the eluent. The pure product **9** (0.061 g, 66%) was isolated as a white powder; mp 72–75 °C (Found: C, 86.54; H, 8.43. Calc. for $C_{28}H_{34}O$: C, 86.99; H, 8.86%); ν_{max}(KBr)/cm^{-1} 3411, 3038, 2920, 2849, 1465, 1057 and 843; δ_H/ppm (250 MHz; $CDCl_3$) 1.18 (1 H, br s), 1.28 (17 H, br s), 1.53 (2 H, m), 1.86 (2 H, q, *J* 8.0 Hz), 3.34 (2 H, t, *J* 7.8 Hz), 3.63 (2 H, t, *J* 6.8 Hz), 7.87 (1 H, d, *J* 7.8 Hz), 7.93–8.20 (7 H, m) and 8.29 (1 H, d, *J* 9.3 Hz); δ_C(63 MHz; $CDCl_3$) 25.96, 29.64, 29.81, 30.05, 32.17, 33.05, 33.84, 63.33, 123.77, 124.82, 124.99, 125.33, 125.97, 126.69, 127.29, 127.47, 127.77, 128.85, 129.93, 131.20, 131.71 and 137.60; HRMS: *m*/*z* (TOF-ES+) 409.1206 (Calc. for $C_{28}H_{34}ONa$: 409.2507).

1-(Pyren-1-yl)dodecane-1,12-diol (10). 12-Oxo-12-(pyren-1-yl)dodecanoic acid **5a** (0.1 g, 0.24 mmol) was dissolved in 1 mL of dry THF. This solution was added dropwise to a stirring suspension of LAH (0.09 g, 2.4 mmol) in 1 mL of dry THF. The resulting mixture was stirred for 5–6 h at RT. After the reaction, excess of LAH was neutralized by addition EtOAc and moist EtOH. The mixture was filtered. Filtrate was concentrated and dried. The crude product was further purified by column chromatography over Merck silica 60 column using EtOAc–DCM (5 : 95) as eluent. The pure product **10** (0.068 g, 70%) was isolated as a pale yellow powder; mp 111–112 °C (Found: C, 76.29; H, 8.93. Calc. for $C_{28}H_{34}O_2 + 2\,H_2O$: C, 76.67; H, 8.73%); ν_{max}(KBr)/cm^{-1} 3415, 2920, 2850, 1465, 1057 and 843; δ_H/ppm (250 MHz; $CDCl_3$) 1.25 (14 H, br s), 1.54 (2 H, m), 2.05 (2 H, m), 3.62 (2 H, t, *J* 6.5 Hz), 5.80 (1 H, t, *J* 6.3 Hz), 7.97–8.21 (8 H, m) and 8.37 (1 H, d, *J* 9.5 Hz); δ_C/ppm (63 MHz; $CDCl_3$) 25.94, 26.47, 29.61, 29.73, 29.76, 29.81, 33.04, 39.42, 63.33, 71.68, 122.81, 123.57, 125.16, 125.22, 125.29, 125.46, 126.16, 127.42, 127.73, 127.79, 127.83, 130.86, 130.94, 131.67 and 138.69; HRMS: *m*/*z* (TOF-ES+) 425.2405 (Calc. for $C_{28}H_{34}O_2Na$: 425.2457).

1,1′-(Dodecane-1,12-diyl)dipyrene (11). To a reaction mixture containing pyrene (10.1 g, 0.05 mol) and dodecanedioyl dichloride (7 g, 0.026 mol; see **5a**) in dichloroethane (150 ml) was cooled in an ice bath for 15 min. To this stirred solution $TiCl_4$ (40 g, 0.2 mol) was added dropwise during 4 h at 5 °C or lower temperature. The dark brown complex formed was allowed to warm to room temperature. The stirring was continued until the pyrene disappeared by TLC. The complex was cleaved by the addition of water and the product was extracted into $CHCl_3$ in Soxhlet apparatus and washed with water (2 × 50 ml) and dried over anhydrous $MgSO_4$. The solvent was removed under reduced pressure yielding a mixture of impure 1,12-di(pyren-1-yl)dodecane-1,12-dione and 12-

oxo-12-(pyren-1-yl)dodecanoic acid **5a**, which were used as such in the next reaction.

200 ml of digol was added with KOH (25 g, 0.45 mol) and the mixture was heated to 180 °C under a nitrogen purge. Hydrazine hydrate (10 ml, 0.2 mol) was added dropwise keeping the temperature above 180 °C under 20 h. After all the hydrazine was added, the temperature was raised to 220 °C for 4 h under nitrogen flush and the mixture was cooled to 50 °C. Hexane (5 × 500 ml) was added and refluxed for 20 minutes under vigorous stirring for each batch. The hexane phase was separated and mixed with 10 g of silica, filtered and evaporated under reduced pressure to 20 ml and then let evaporate to dryness slowly at normal pressure in a flask in a hood. Colourless crystalline powder of **11** (2.2 g, 15%) was obtained.

The digol phase was neutralized with 10% HCl and extracted with chloroform (3 × 250 ml). The chloroform was washed with 2 × 100 ml of water and dried over $MgSO_4$. 75 g of silica was added to the chloroform and the solvent was evaporated to dryness under reduced pressure. The silica was eluted with THF–hexane–methanol (19 : 80 : 1) over 1.5 kg of Merck silica 60 in a preparative MPLC. The pure product **5** (3.5 g, 18%) was recovered.

1,1′-(dodecane-1,12-diyl)dipyrene **11** (2.2 g, 15%); mp 129–132 °C (Found: C, 92.57; H, 7.49. Calc. for $C_{44}H_{42}$: C, 92.58; H, 7.42%); ν_{max}(KBr)/cm^{-1} 3038, 2918, 2851, 1604, 1466, 1418, 1180, 963, 844, 758, 723, 706, 681 and 620; δ_H(500 MHz; $CDCl_3$) 1.28 (8 H, m), 1.37 (4 H, m), 1.48 (4 H, q), 1.82 (4 H, q), 3.33 (4 H, t), 7.86 (2 H, d, *J* 8.0 Hz), 7.96–8.03 (6 H, m), 8.08–8.16 (8 H, m) and 8.28 (2 H, d, *J* 9.5 Hz); δ_C(126 MHz; $CDCl_3$) 29.556, 29.580, 29.607, 29.802, 31.926, 33.602, 123.536, 124.583, 124.746, 124.758, 125.107, 125.120, 125.726, 126.455, 127.058, 127.226, 127.531, 128.631, 129.701, 130.974, 131.486 and 137.374; HRMS: *m*/*z* (EI 70 eV) 570.3280 (Calc. for C44H42: 570.3287).

Acknowledgements

This work was supported by the Academy of Finland grants 106998 and 107014. Thanks are due to Paavo Niutanen for his help in SEM sample preparation, to Reijo Kauppinen for NMR and to Mirja Lahtiperä for MS. We also thank Dr Roland Pein at DLR, Lampoldshausen, Germany for providing facilities for rheometry and Prof. Uday Maitra IISc, Bangalore, India for equipment for UV/Vis and fluoresence spectroscopy.

References

1. (*a*) N. M. Sangeetha and U. Maitra, *Chem. Soc. Rev.*, 2005, **34**, 821–836; (*b*) 'Low Molecular Mass Gelators', in *Topics in Current Chemistry*, ed. F Fages, Springer, Berlin, Heidelberg, 2005, vol. 256; (*c*) *Molecular Gels: Materials with Self-Assembled Fibrillar Networks*, ed. R. G. Weiss and P Terech, Springer, Dordrecht, 2006; (*d*) P. Terech and R. G. Weiss, *Chem. Rev.*, 1997, **97**, 3133–3159; (*e*) L. A. Estroff and A. D. Hamilton, *Chem. Rev.*, 2004, **104**, 1201–1217.
2. (*a*) J. H. van Esch and B. L. Feringa, *Angew. Chem., Int. Ed.*, 2000, **39**, 2263–2266; (*b*) G. Mieden-Gundert, L. Klein, M. Fischer, F. Vögtle, K. Heuzé, J. L. Pozzo, M. Vallier and F. Fages, *Angew. Chem., Int. Ed.*, 2001, **40**, 3164–3166; (*c*) S. Tamaru, M. Nakamura, M. Takeuchi and S. Shinkai, *Org. Lett.*, 2001, **3**, 3631–3634.
3. (*a*) K. J. C. van Bommel, A. Friggeri and S. Shinkai, *Angew. Chem., Int. Ed.*, 2003, **42**, 980; (*b*) C. L. Chan, J. B. Wang, J. Yuan, H. Gong, Y. H. Liu and M. H. Liu, *Langmuir*, 2003, **19**, 9440; (*c*) C. S. Love, V. Chechik, D. K. Smith, K. Wilson, I. Ashworth and C. Brennan, *Chem. Commun.*, 2005, 1971; (*d*) K. Sugiyasu, S. Tamura, M. Takeuchi, D. Berthier, I. Huc, R. Oda and S. Shinkai, *Chem. Commun.*, 2002, **1212**; (*e*) S. Kobayashi, N. Hamasaki, M. Suzuki, M. Kimura, H. Shirai and K. Hanabusa, *J. Am. Chem. Soc.*, 2002, **124**, 6550; (*f*) E. D. Sone, E. R. Zubarev and S. I. Stupp, *Angew. Chem. Int., Ed.*, 2002, **41**, 1705; (*g*) Z. Hu and X. Xia, *Adv. Mater.*, 2004, **16**, 305; (*h*) M. Kimura, S. Kobayashi, T. Kuroda, K. Hanabusa and H. Shirai, *Adv. Mater.*, 2004, **16**, 335; (*i*) M. Asai, K. Sugiyasu, N. Fujita and S. Shinkai, *Chem. Lett.*, 2004, **33**, 120; (*j*) B. Simmons, S. Li, V. T. John, G. L. McPherson, C. Taylor, D. K. Schwartz and K. Maskos, *Nano Lett.*, 2002, **2**, 1037.
4. (*a*) A. Bögershausen, S. J. Pas, A. J. Hill and H. Koller, *Chem. Mater.*, 2006, **18**, 664–672; (*b*) S. J. Langford, M. J. Latter, V.-L. Lau, L. L. Martin and A. McChler, *Org. Lett.*, 2006, **7**, 1371–1373; (*c*) H. Jung, S. J. Lee, J. A. Rim, H. Lee, T.-S. Bae, S. S. Lee and S. Shinkai, *Chem. Mater.*, 2005, **17**, 459–462; (*d*) S. Milijanic, L. Frkanec, Z. Meic and M. Zinic, *Langmuir*, 2005, **21**, 2754–2760; (*e*) S. J. Lee, S. S. Lee, J. S. Kim, J. Y. Lee and J. H. Jung, *Chem. Mater.*, 2005, **17**, 6517–6520; (*f*) A. Kishimura, T. Yamashita and T. Aida, *J. Am. Chem. Soc.*, 2005, **127**, 179–183; (*g*) S. H. Seo and J. Y. Chang, *Chem. Mater.*, 2005, **17**, 3249–3254; (*h*) Y. Watanabe, T. Miyasou and M. Hayashi, *Org. Lett.*, 2004, **6**, 1547–1550; (*i*) M. George, S. L. Snyder, P. Terech, C. J. Glinka and R. G. Weiss, *J. Am. Chem. Soc.*, 2003, **125**, 10275–10283; (*j*) A. Friggeri, O. Gronwald, K. J. C. van Bommel, S. Shinkai and D. N. Reinhoudt, *J. Am. Chem. Soc.*, 2002, **124**, 10754–10758; (*k*) M. George and R. G. Weiss, *J. Am. Chem. Soc.*, 2001, **123**, 10393–10394; (*l*) A. Ajayaghosh and S. J. George, *J. Am. Chem. Soc.*, 2001, **123**, 5148–5149; (*m*) D. J. Abdallah, L. Lu and R. G. Weiss, *Chem. Mater.*, 1999, **11**, 2907–2911; (*n*) K. Hanabusa, K. Hiratsuka, M. Kimura and H. Shirai, *Chem. Mater.*, 1999, **11**, 649–655; (*o*) P. Terech and R. G. Weiss, *Chem. Rev.*, 1997, **97**, 3133–3160; (*p*) S. Ray, A. K. Das and A. Banerjee, *Chem. Commun.*, 2006, 2816–2818; (*q*) X.-Q. Li, V. Stepanenko, Z. Chen, P. Prins, L. D. A. Sibbeles and F. Würthner, *Chem. Commun.*, 2006, 3871–3873.
5. (*a*) P. Babu, N. M. Sangeetha, P. Vijaykumar, U. Maitra, K. Rissanen and A. R. Raju, *Chem.–Eur. J.*, 2003, **9**, 1922–1932; (*b*) U. Maitra, P. Vijaykumar, N. M. Sangeetha, P. Babu and A. R. Raju, *Tetrahedron: Asymmetry*, 2001, **12**, 477–480.
6. M. J. Frisch, G. W. Trucks, H. B. Schlegel, G. E. Scuseria, M. A. Robb, J. R. Cheeseman, J. A. Montgomery Jr, T. Vreven, K. N. Kudin, J. C. Burant, J. M. Millam, S. S. Iyengar, J. Tomasi, V. Barone, B. Mennucci, M. Cossi, G. Scalmani, N. Rega, G. A. Petersson, H. Nakatsuji, M. Hada, M. Ehara, K. Toyota, R. Fukuda, J. Hasegawa, M. Ishida, T. Nakajima, Y. Honda, O. Kitao, H. Nakai, M. Klene, X. Li, J. E. Knox, H. P. Hratchian, J. B. Cross, V. Bakken, C. Adamo, J. Jaramillo, R. Gomperts, R. E. Stratmann, O. Yazyev, A. J. Austin, R. Cammi, C. Pomelli, J. W. Ochterski, P. Y. Ayala, K. Morokuma, G. A. Voth, P. Salvador, J. J. Dannenberg, V. G. Zakrzewski, S. Dapprich, A. D. Daniels, M. C. Strain, O. Farkas, D. K. Malick, A. D. Rabuck, K. Raghavachari, J. B. Foresman, J. V. Ortiz, Q. Cui, A. G. Baboul, S. Clifford, J. Cioslowski, B.B. Stefanov, G. Liu, A. Liashenko, P. Piskorz, I. Komaromi, R. L. Martin, D. J. Fox, T. Keith, M. A. Al-Laham, C. Y. Peng, A. Nanayakkara, M. Challacombe, P. M. W. Gill, B. Johnson, W. Chen, M. W. Wong, C. Gonzalez, J. A. Pople, *GAUSSIAN 03 (Revision C.02)*, 2004, Gaussian, Inc., Wallingford, CT, 2001.
7. C. A. Hunter, K. R. Lawson, J. Perkins and C. J. Urch, *J. Chem. Soc., Perkin Trans. 2*, 2001, 651–669.
8. (*a*) Cook and Hewett, *J. Chem. Soc.*, 1933, 398–401; Cook and Hewett, *Chem. Ind. (London)*, 1936, 843; Winterstein, Vetter and Schoen, *Chem. Ber.*, 1935, **68**, 1079–1082; Bachmann, Carmack and Safir, *J. Am. Chem. Soc.*, 1941, **63**, 1682–1684; (*b*) S. Katusin-Razem, *Croat. Chem. Acta*, 1978, **51**, 163–164.